EurJOC European Journal of Organic Chemistry

FULL PAPER

DOI: 10.1002/ejoc.201300192

D–π–A Dye Sensitizers Made of Polymeric Metal Complexes Containing 1,10-Phenanthroline and Alkylfluorene or Alkoxybenzene: Synthesis, Characterization and Photovoltaic Performance for Dye-Sensitized Solar Cells

Xiaoguang Yu,[a] Xueliang Jin,[a] Guipeng Tang,[a] Jun Zhou,[a] Wei Zhang,[a] Dahai Peng,[a] Jiaomei Hu,[a] and Chaofan Zhong*[a]

Keywords: Polymeric metal complex / Dye-sensitized solar cells / Energy conversion / Ligand design / Donor–acceptor systems

Four polymeric metal complexes (**P1**–**P4**) based on 1,10-phenanthroline metal complexes and alkylfluorene or alkoxybenzene were synthesized by the Heck coupling reaction and were developed for dye-sensitized solar cell applications. The target dyes use alkoxybenzene or alkylfluorene as the electron donor, a C=C moiety as the π linker, and the phenanthroline derivative complex was used as the electron acceptor. Bipyridine derivatives were ancillary ligands as well as providing anchoring groups. The thermal, photophysical, electrochemical and photovoltaic properties of these copolymers were investigated by thermogravimetric analysis (TGA), differential scanning calorimetry (DSC), C–V curves and I–V curves. Dye-sensitized solar cells with these polymeric metal complexes as dye sensitizers exhibited considerable power conversion efficiencies (PCE). The dyes containing alkoxybenzenes (**P3**, **P4**) exhibited higher PCE values than the corresponding target polymers containing alkylfluorenes (**P1**, **P2**), The dye **P3** showed the maximal power conversion efficiency of 2.12 % (J_{sc} = 4.91 mA/cm^2, V_{oc} = 0.69 V, FF = 62.5). In addition, the four polymers possessed excellent stabilities, and their thermal decomposition temperatures all exceeded 300 °C, indicating that these polymeric metal complexes are suitable for the fabrication processes of optoelectronic devices.

Introduction

In recent decades, because of the rapid depletion of conventional energy sources and the increasing emission of greenhouse gases, the development of dye-sensitized solar cells (DSSCs) has been paid increasing attention, mainly due to their potential ease of fabrication, abundant material sources, and cost effectiveness compared with silicon-based photovoltaic devices.[1] After two decades of research and development, DSSCs based on ruthenium dyes have achieved record light-to-electric power conversion efficiencies of over 11%, and over 10% based on metal-free organic dyes since the first demonstration in 1991 by O'Regan and Grätzel.[2] Many recent efforts have been devoted to designing and synthesizing efficient dye sensitizers that are suitable for practical use.

The typical DSSC is composed of a photoanode and a photoinert counterelectrode (cathode) sandwiching a redox mediator. It consists of five materials: (1) a fluorine-doped SnO_2 (FTO) glass substrate, (2) a nanocrystalline TiO_2 thin film as a semiconductor, (3) a dye sensitizer, (4) an electrolyte (redoxmediator), and (5) a platinum-coated glass substrate.[3] One of the key roles in DSSCs is attributed to the sensitizers, which are responsible for light absorption and the generation of electric charges.[4] So far, much effort has been put forth in the development of various types of organic dye sensitizers for DSSCs. There are two kinds of dyes, namely, metal–organic complexes and metal-free organic dyes. Typical metal–organic dyes are a class of polypyridyl complexes of ruthenium, such as N3,[5] N719,[6] and "black dye".[7] These dyes are already commercially available. Other polymeric dyes including K19,[8] C101,[9] and CYC-B11,[10] have also been reported to have high efficiencies of 10–11%. Ru complexes as dyes were extensively researched in DSSCs. The ruthenium complex dyes have been distinguished by attaining more than 11% efficiencies under simulated air mass 1.5 global sunlight. However, Ru-complex dyes have met with some problems, such as limited resources, difficult purification, and environmental pollution. Therefore, dye sensitizers containing common metals have attracted interest because of their modest cost, convenience of customized molecular design, and ease of synthesis. Aswani Yella and coworkers discovered a zinc (Zn) porphyrin dye with a cobalt (II/III)-based redox electrolyte leading to record power conversion efficiency approaching 13% under simulated air mass 1.5 global sunlight.[11] This demonstrates that common-metal dye sensitizers can achieve the same high efficiency as ruthenium complexes.

[a] Key Laboratory of Environmentally Friendly Chemistry and Applications of Ministry of Education, Xiangtan University, College of Chemistry,
Xiangtan, Hunan 411105, P. R. China
E-mail: zhongcf798@yahoo.com.cn
Homepage: http://hxxy.web.xtu.edu.cn:8081/

Supporting information for this article is available on the WWW under http://dx.doi.org/10.1002/ejoc.201300192.

 © 2013 Wiley-VCH Verlag GmbH & Co. KGaA, Weinheim

The polymeric metal-complex dyes have their own advantages, such as good thermal stability, processability, and easy film-forming ability. Because hybrid polymers containing inorganic and organic segments exhibit properties of both inorganic and organic-metal complexes, they are likely to meet requirements of highly efficient DSSCs, and many hybrid polymers have been investigated and used for DSSCs.[12] Among these hybrid polymer dyes, the D–π–A structure is the common motif[13–19] because of its intramolecular charge transfer characteristics.[20]

The important ligand, 1,10-phenanthroline (phen), is one of the most widely used chelating ligands in modern coordination chemistry.[21] The unit has a rigid structure, high electron transfer capability, and can provide two aromatic nitrogens, which allow it to coordinate with many transition metal ions easily. Considering the distinctive physical and chemical properties of phenanthroline, some researchers have used metal–phenanthroline-derivative complexes in DSSCs. For instance, Jen-Fu Yin and co-workers discovered that [Ru(dcbpy)(otip)(NCS_2)][22] containing a thiophene-substituted spacer, has achieved an energy efficiency of 8.3%. Kohjiro Hara and coworkers discovered that [Ru(dcphen)$_2$(NCS_2)][23] containing *cis*-dithiocyanatobis-(4,7-dicarboxy-1,10-phenanthroline) obtained an energy efficiency of 6.1%, and the similar dye CYC-P1[24] has achieved an energy efficiency of 6.01% in DSSCs. To achieve high quantum yields for the excited-state electron-transfer process, the dye needs to have at least one anchoring group for adsorption onto the TiO_2 surface. The anchor group can bind the molecules to the surface and inject the electrons from the excited dye molecule to the conducting band of the semiconductor. 3,3′-Dicarboxy-2,2′-bipyridine is an excellent polydentate ligand, and has been widely used in spectroscopic, electrochemical, and magnetic applications.[25]

In this article, four polymeric metal complexes (**P1**–**P4**) with D–π–A structures[26] were synthesized. In these complexes, the phenanthroline derivative part was used as the electron acceptor, a C=C moiety was used as the π linker, and an alkoxybenzene or an alkylfluorene group was used as the electron donor. Zn^{II} or Co^{II} was chosen as the metal, each for its interesting charge properties and low cost. Bipyridine derivatives served as ancillary ligands, as well as providing anchoring groups. The introduction of alkoxy or alkyl groups to the molecules in question was to improve the solubility of the polymers. The photophysical and thermal properties of the four polymeric metal complexes were studied, and the performance of DSSCs based on these four dyes as photosensitizers was investigated in detail.

Results and Discussion

Synthesis and Characterization

Scheme 1 shows the synthetic routes to the metal complexes **L1** and **L2**, as well as to the four main-chain poly-

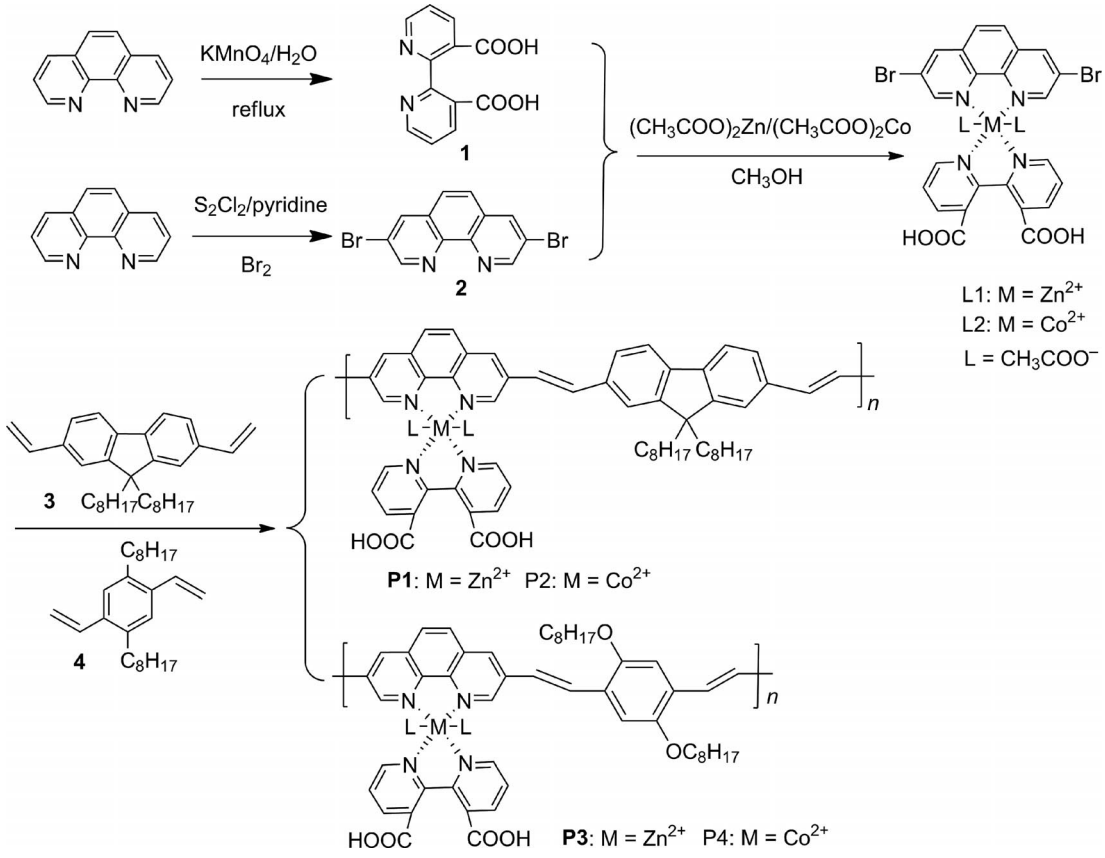

Scheme 1. Synthesis of the monomers **L1**, **L2** and four polymeric metal complexes (**P1–P4**).

 © 2013 Wiley-VCH Verlag GmbH & Co. KGaA, Weinheim

meric metal complexes (**P1**–**P4**), which were synthesized by the Heck coupling.[27]

The IR spectra of the ligand–metal complexes **L1** and **L2** and the target polymers (**P1**–**P4**) are shown in Figure 1. In parts a and b of Figure 1 there is a broad absorption band at 3500–3280 cm^{-1}, which is attributable to the existence of lattice and/or coordinated water in the molecule. The presence of these water molecules makes it difficult to see underlying bands due to the O–H stretching vibrations.[28] We can see that there are weak peaks around 3037 cm^{-1}, which can be attributed to the aromatic CH stretching vibrations for all the compounds. The peaks at 1113 and 1107 cm^{-1} are due to C–O vibrations at the C–O–M sites of the acetate ligands[29] of metal compounds **L1** and **L2**. Accordingly, the M–N stretching vibration peaks of metal compounds appear at 559 and 554 cm^{-1} for ligands **L1** and **L2**, respectively.[30]

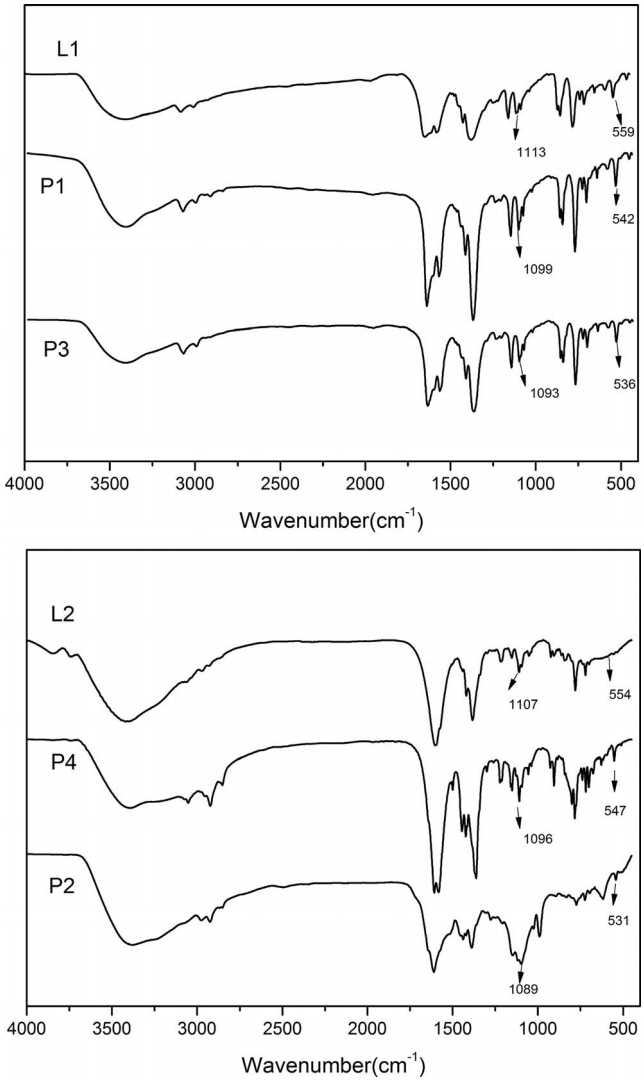

Figure 1. Top: FTIR spectra of **L1** and polymeric metal complexes (**P1**, **P3**). Bottom: FTIR spectra of **L2** and polymeric metal complexes (**P2**, **P4**).

Gel permeation chromatography (GPC) results of all the target polymers are shown in Table 1. The average molecular weights of **P1**–**P4** are 12.01, 9.7, 13.0 and 7.9 kg/mol, respectively, with relative polydispersity indexes (PDI) in the range of 1.26–1.53. These results, combined with elemental analysis, indicate that polymerization has taken place between monomers, which also proved that the target polymeric dyes have been obtained.

Table 1. Polymerization results, thermal and optical properties of polymers **P1**–**P4**.

Polymer	*M*n [$\times 10^3$]	*M*w [$\times 10^3$]	PDI	*n*	T_d [°C][a]	T_g [°C][b]
P1	11.8	13.5	1.53	11	311	138
P2	9.6	13.7	1.41	9	287	119
P3	13.4	16.3	1.26	13	376	147
P4	10.3	13.8	1.39	10	357	141

[a] The data were obtained from TGA of the polymeric metal complexes. [b] Glass transition temperatures, measured from DSC traces of the polymeric metal complexes.

Optical Properties

The UV/Vis and normalized photoluminescent (PL) spectra of the metal complexes **L1** and **L2**, and the polymeric metal complexes **P1**–**P4** (10^{-5} M in DMF solution) are shown in Figures 3 and 4. The corresponding data are summarized in Table 2.

Table 2. The optical properties of metal complexes **L1** and **L2** and polymeric metal complexes **P1**–**P4**.

	UV/Vis absorbance, $\lambda_{a,max}$ [nm][a]	PL, $\lambda_{p,max}$ [nm]
2	352	
L1	319, 358	
L2	317, 363	
P1	411	474
P2	396	486
P3	442	498
P4	424	491

[a] $\lambda_{a,max}$: The maxima and onset absorption from the UV/Vis spectra in DMF solution. $\lambda_{p,max}$: The PL maxima in DMF solution.

Figure 2 shows the UV/Vis spectra of the metal complexes **L1** and **L2**. The light absorption of metal complexes **L1** and **L2** is primarily attributable to metal-to-ligand charge transfer (MLCT). The absorption maxima of the complexes are concentrated in the ultraviolet and near-ultraviolet regions. In Figure 3, we can observe that the absorption maxima of **P1**–**P4** are at 411, 396, 442, and 424 nm, respectively. These strong absorption bands result from intramolecular charge transfer (ICT) between the electron-acceptor–metal-phenanthroline unit and the electron-donating alkoxybenzene or alkylfluorene moiety. In comparison with the π-π* transition absorption of the monomer **2** phenanthroline ring, the maximum absorptions of the polymeric metal complexes (**P1**–**P4**) are obviously red-shifted due to the introduction of the fluorene or phenylene

 © 2013 Wiley-VCH Verlag GmbH & Co. KGaA, Weinheim

donor unit and coordination of the ligand with metal. The absorption spectra of the polymers are wider, but maximum absorption wavelengths are still short, which may be extremely unfavorable to improving dye-sensitized solar cells' energy conversion efficiency. Therefore, the proportion of the donor groups should be improved in order to modify the structure of polymeric metal complexes containing this kind phenanthroline derivative.

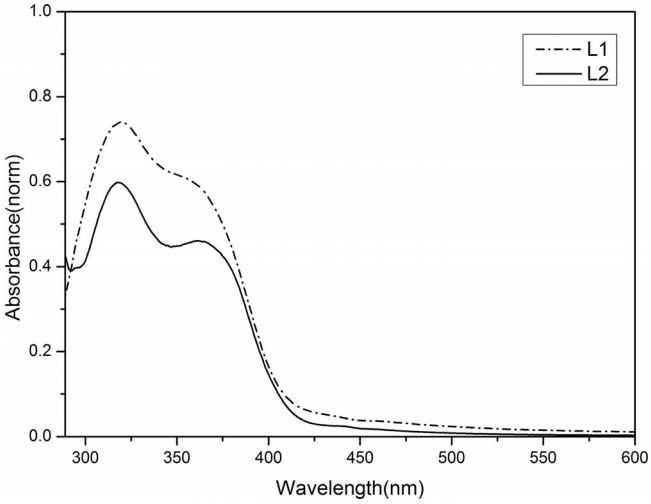

Figure 2. Normalized absorption spectra of metal complexes **L1** and **L2**.

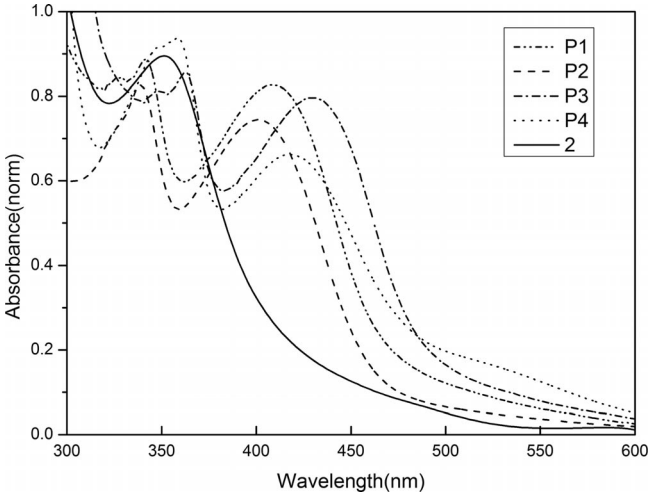

Figure 3. Normalized absorption spectra of the ligand **2** and polymeric metal complexes **P1**–**P4**.

The normalized photoluminescent spectra of **P1**–**P4** in DMF solution are shown in Figure 4. The excitation wavelengths were set according to the absorption peak of UV/Vis spectrum, and the corresponding optical data are also listed in Table 2. It can be seen that the PL peaks of **P1**–**P4** are at 474, 486, 498and 491 nm, respectively, which can be attributed to the π-π* transition of each ligand moiety.

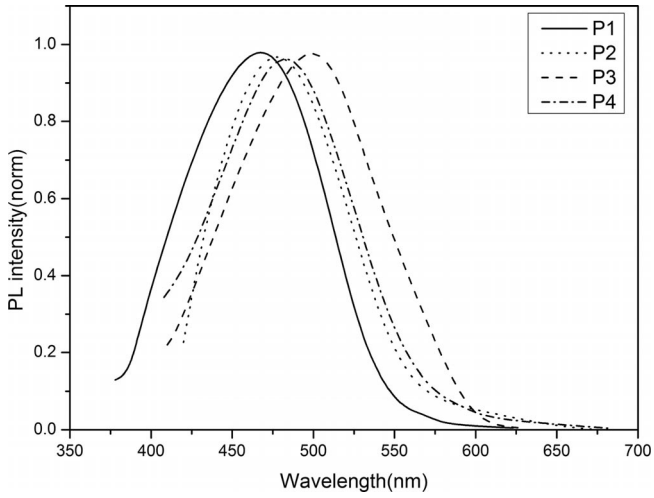

Figure 4. PL spectra of the four polymeric metal complexes **P1**–**P4**.

Thermal Stability

Stability is an important consideration in the design of dye-sensitized solar cells. The dye should have good stability, which can significantly improve the working life of the photovoltaic devices. Therefore, the thermal stability study has important implications for DSSCs. The thermal properties of these four polymeric metal complexes were studied by TGA and DSC . The TGA traces are shown in Figure 5, and the corresponding data are listed in Table 1. The TGA data show the T_d values (5% weight-loss temperature of the product) of the four polymeric metal complexes (**P1**–**P4**) at temperatures of 311, 376, 287 and 357 °C, respectively, under nitrogen, which means all of them are steady.[31] From the data of Table 1, we can see that the

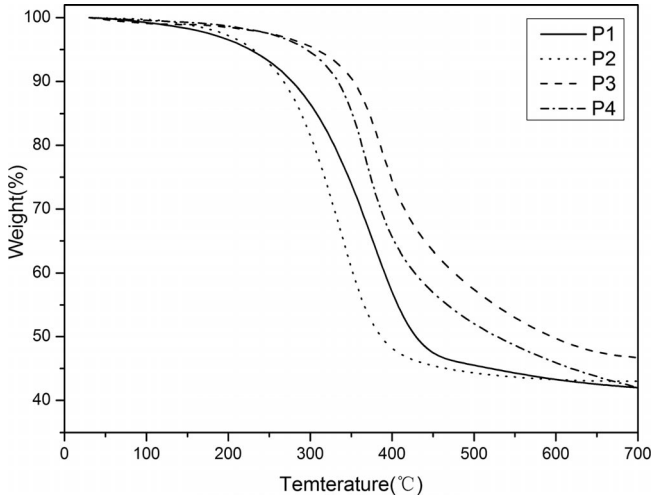

Figure 5. TGA curves of **P1**–**P4** with a heating rate of 20 °C/min under nitrogen atmosphere.

 © 2013 Wiley-VCH Verlag GmbH & Co. KGaA, Weinheim

glass transition temperatures (T_g) of the four polymeric metal complexes (**P1**–**P4**) follow the order **P3** (147 °C) > **P4** (141 °C) > **P1** (138 °C) > **P2** (119 °C). The results imply that alkoxybenzene units hold higher rigidity than do alkylfluorene units. There is no fixed melting point, which means the polymers are amorphous. The amorphous nature of the polymers might serve as a drawback for their use in organic solar cells.[32] On the other hand, their high glass-transition temperature shows that these kinds materials may provide the solar cell device with greater longevity.[33]

Electrochemical Properties

The highest occupied molecular orbital (HOMO) and lowest unoccupied molecular orbital (LUMO) energy levels of the dyes are important parameters in the design of optoelectronic devices, and they can be estimated by cyclic voltammetry (CV). When a saturated calomel electrode (SCE) is used as the reference electrode, the HOMO and LUMO energy levels can be calculated from the onset oxidation potentials (E_{ox}) and the onset reduction potentials (E_{red}) of the polymers according to Equations (1), (2) and (3), respectively.[34,35]

$$\text{HOMO} = -e(E_{ox} + 4.40)\ (\text{eV}) \quad (1)$$

$$\text{LUMO} = -e(E_{red} + 4.40)\ (\text{eV}) \quad (2)$$

$$E_g = \text{HOMO} - \text{LUMO} \quad (3)$$

The cyclic voltammograms of the dyes were measured in DMF solution containing $[Bu_4N]BF_6$ as a supporting electrolyte, and a SCE as the reference electrode at a scan rate of 100 mV/s. Figure 6 shows cyclic voltammetry curves of **P1**–**P4**, and the corresponding CV data are summarized in Table 3. The E_{ox} values were observed to be 1.26, 1.32, 1.15, and 1.18 V for **P1**, **P2**, **P3** and **P4**, respectively. On the other hand, their onset potentials for reduction (E_{red}) were found to be –1.02, –1.04, –0.98, –1.05 V, respectively. Accordingly, the HOMO energy levels of **P1**, **P2**, **P3** and **P4**, are –5.66 eV, –5.72 eV, –5.55 eV and –5.58 eV, respectively, which are much lower than the standard potential of the I_3/I^- redox couple (–4.83 eV vs. vacuum).[36] This difference indicates that the dyes will be more effectively regenerated, and suppress the recapture of the injected electrons by the dye cation radical.[37] The LUMO energy levels of **P1**–**P4** are sufficiently higher than the conduction band of (–4.0 eV)[38] to imply the possibility of an effective charge transfer from the polymers to TiO_2.[39] The E_g values of **P1**–**P4** followed the order of **P2** (2.36 eV) > **P1** (2.28 eV) > **P4** (2.23 eV) > **P3** (2.13 eV). We found that the E_g values of polymeric metal complexes containing alkoxybenzene donor units were lower than those of the corresponding polymeric metal complexes containing alkylfluorene donor units, which indicated that the stronger electron-donating ability of alkoxybenzene units decreased the energy gap.

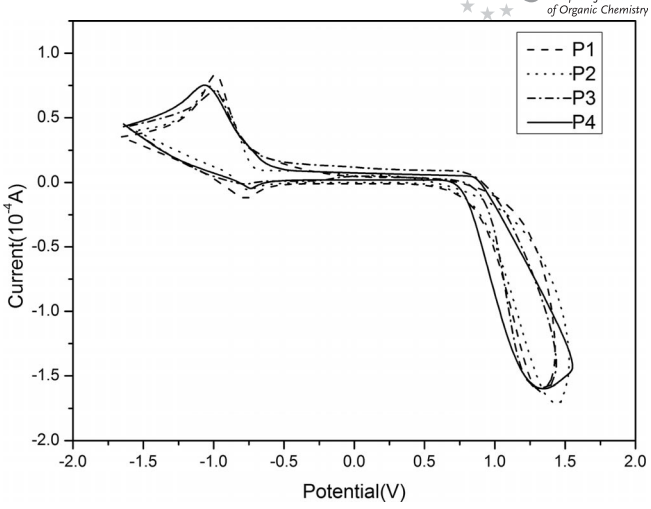

Figure 6. CV curves of **P1**–**P4** measured in DMF solution containing $[Bu_4N]BF_6$ as supporting electrolyte at a scan rate of 100 mV/s.

Table 3. Cyclic voltammetry results of polymeric metal complexes **P1**–**P4**.

Polymer	E_{red} [V]	E_{ox} [V]	HOMO [eV]	LUMO [eV]	E_g [eV]
P1	–1.02	1.26	–5.66	–3.28	2.28
P2	–1.04	1.32	–5.72	–3.36	2.36
P3	–0.98	1.15	–5.55	–3.42	2.13
P4	–1.05	1.18	–5.58	–3.35	2.23

Photovoltaic Properties

The incident photo-to-current conversion efficiency (IPCE) plots for the DSSCs based on **L1**, **L2**, and **P1**–**P4** are shown in Figures 7 and 8. The two metal complexes responded in the broad range of 350–400 nm, and the maximum IPCE values were around 5%, which is very low. The four polymer dyes all responded in the broad range of 400–650 nm and showed maximum IPCE values around 420 nm, which was in accord with the UV/Vis spectra. The IPCE values of the dyes **P1**–**P4** reached 35.1% to 38.3%. Among the four target dyes, **P3** had the maximum IPCE, possibly because it had the largest adsorption onto the TiO_2 film. This indicates that dye **P3** would show a relatively high photocurrent in DSSCs.

The photovoltaic characteristics of DSSCs based on the two metal complexes and four polymer dyes are shown in Figures 9 and 10. The corresponding open-circuit voltage (V_{oc}), short-circuit current density (J_{sc}), fill factor (FF) and power conversion efficiency (PCE) values are listed in Table 4. As can be observed, DSSCs based on metal complexes **L1** and **L2** generated very low power conversion efficiencies (0.15% and 0.11%), which indicates that due to the limited solubility of the complexes, the monomeric complexes can not obtain good photoelectric conversion efficiencies. Metal complexes **L1** and **L2** bonded with the donor moieties by the Heck coupling reaction to form four

 © 2013 Wiley-VCH Verlag GmbH & Co. KGaA, Weinheim

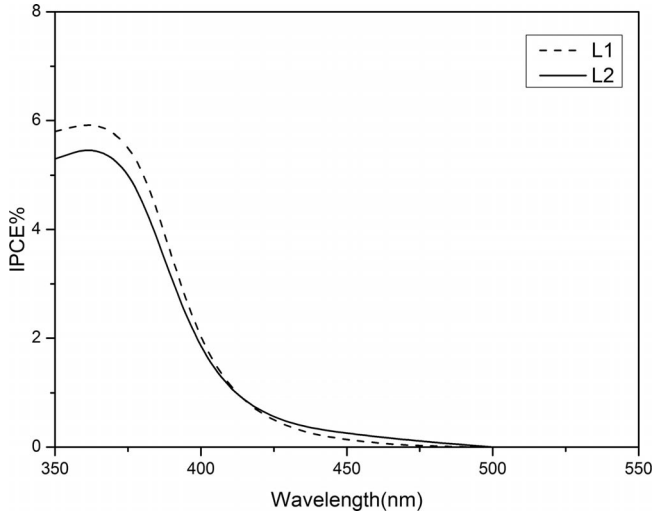

Figure 7. Incident photon-to-current conversion efficiency of metal complexes **L1** and **L2**.

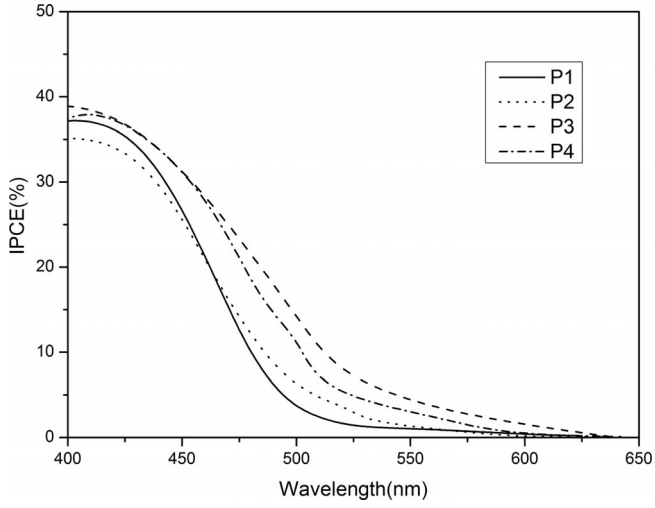

Figure 8. Incident photon-to-current conversion efficiency of the four polymeric metal complexes **P1**–**P4**.

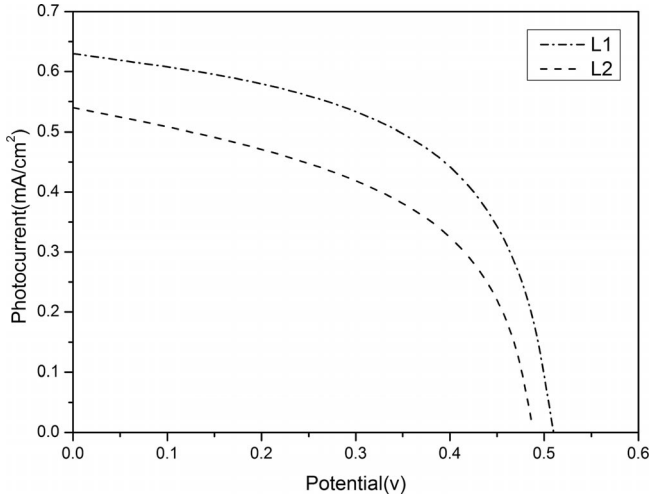

Figure 9. J-V curves of DSSCs based on **L1**, and **L2** in DMF solution.

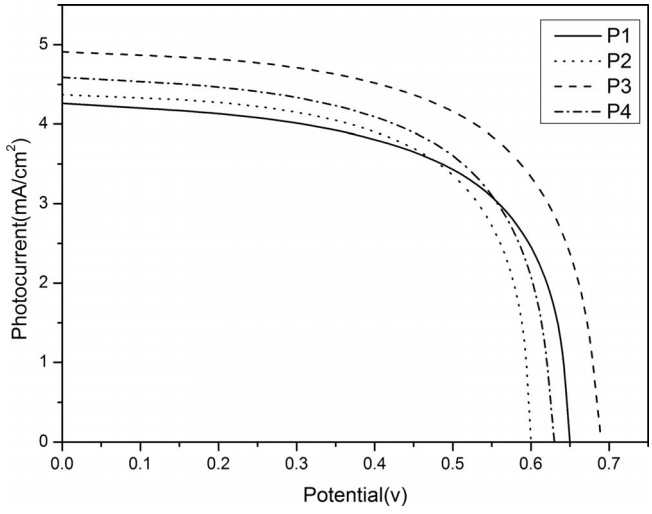

Figure 10. J-V curves of DSSCs based on **P1**–**P4** in DMF solution.

target polymer dyes. The formation of polymers extended the conjugated chains, tuned the energy gap between the donor part and acceptor parts, thus reducing the energy gap, and effectively improving the photovoltage and photocurrent of the target products. As expected, the polymer metal complex dyes showed a better photovoltaic performances than those of metal complexes **L1** and **L2**.

Further study showed that the V_{oc} values of **P1**–**P4** dyes are 0.65 V, 0.69 V, 0.60 V, 0.64 V, respectively, and the corresponding FF values are 0.636, 0.625, 0.650 and 0.614. The J_{sc} values follow the order **P3** (4.91 mA/cm^2) > **P4** (4.59 mA/cm^2) > **P2** (4.37 mA/cm^2) > **P1** (4.26 mA/cm^2). On the basis of the above data, we can see that the J_{sc} values of the target polymers containing alkoxybenzene (**P3**, **P4**) were higher than the corresponding target polymers containing alkylfluorene (**P1**, **P2**), which implies that the alkoxybenzene unit was more conducive to the generation of photocurrent and open circuit voltages than was the octylfluorene unit. The power conversion efficiencies of devices based on **P3** and **P4** reached 1.91%, 1.67%, respectively, which were higher than those of devices based on **P1** (1.76%) and **P2** (1.71%). The results indicate that the d^{10} Zn^{II} complexes possessed higher kinetic stability than did d^7 Co^{II} complexes. Though the power conversion efficien-

Table 4. The data of photovoltaic performances of DSSCs based on **L1**, **L2**, **P1**–**P4** under 1.5 G solar illumination.

Polymer	Solvent	*J*sc [mA cm^{-2}]	V_{oc} [V]	FF [%]	IPCE	η [%]
P1	DMF	4.26	0.65	63.6	37.1%	1.76
P2	DMF	4.37	0.60	65.0	35.1%	1.71
P3	DMF	4.91	0.69	62.5	38.3%	2.12
P4	DMF	4.59	0.64	61.4	37.5%	1.81
L1	DMF	0.63	0.52	46.3	5.8%	0.15
L2	DMF	0.54	0.48	42.5	5.2%	0.11

 © 2013 Wiley-VCH Verlag GmbH & Co. KGaA, Weinheim

cies of the dyes were still low and were not comparable with state-of-the-art ruthenium-based dyes, further work on optimizing the device performance is under investigation.

Conclusions

In conclusion, four D–π–A polymeric metal complexes with phenanthroline–metal complexes as the electron acceptor moieties, C=C π-bridges, and alkoxybenzene or alkylfluorene units as electron donors were designed, synthesized and characterized in DSSCs to obtain efficiency values of up to 2.12%. These results indicate that these polymeric metal complexes have unique advantages as new solar cell materials, and suggest that further structure optimization is essential before application in DSSCs.

For this new type of dye sensitizer there are still many challenges to obtaining outstanding energy conversion efficiencies, for example, the narrow absorption spectra of the polymers, and the low J_{sc} values based on the materials' electron injection efficiency. To improve the conversion efficiencies, we will further design and synthesize new polymeric metal-complex dyes which can broaden the light absorption spectrum in the region of visible light, improve electron transfer efficiency of organic semiconductors and enhance short-circuit current density. Our work towards these goals is under way.

Experimental Section

Instruments and Measurements: All ^1H NMR spectra were obtained in $CDCl_3$ and recorded with a Bruker Avance 400 spectrometer, using tetramethylsilane (δ = 0.00 ppm) as the internal reference. Fourier transform infrared (FTIR) spectra were recorded using KBr pellets (250 mg of dried KBr and 2 mg of lyophilized sample) with a PerkinElmer Spectrum One FTIR spectrometer over the range 400–4000 cm^{-1}. UV/Vis spectra were obtained with a Lambda 25H spectrometer. Samples were dissolved in DMF and diluted to a concentration of 10^{-5}–10^{-4} mol L^{-1}. Photoluminescent spectra (PL) were taken with a Perkin–Elmer LS55 luminescence spectrometer with a xenon lamp as the light source. Gel permeation chromatography (GPC) analyses were performed with a system equipped with a set of Waters HT3, HT4 and HT5 Styragel columns, with THF as the eluent, polystyrene as the standard, and detection using a WATERS 2414 refractive index detector. Thermogravimetric analysis (TGA) was performed with a Shimadzu TGA-7 instrument under nitrogen atmosphere at a heating rate of 20 K min^{-1} from 25 to 600 °C. Differential scanning calorimetry (DSC) was performed using a PerkinElmer DSC-7 thermal analyzer under nitrogen atmosphere at a heating rate of 20 °C min^{-1} from 25 to 600 °C. Cyclic voltammetry (CV) was conducted with a CHI630C Electrochemical Workstation using a three-electrode system in a $[Bu_4N]BF_6$ (0.1 M) DMF solution at a scan rate of 100 mV/s. The working electrode was a glassy carbon electrode, the auxiliary electrode was a platinum wire electrode, and a saturated calomel electrode (SCE) was used as reference electrode.

Fabrication of DSSCs: The DSSC devices with sandwich structure in this paper are based on TiO_2 semiconductors, and their specific production processes are as follows: Titania paste was prepared following a procedure: fluorine-doped SnO_2 conducting glass (FTO) was cleaned and immersed in 40 mM $TiCl_4$ solution at 70 °C for 30 min, then washed with water and ethanol. The TiO_2 colloid comprised of 20–30 nm particles was coated onto the prepared FTO glass by the sliding glass rod method, and was then sintered at 450 °C for 30 min. This process was done three times to obtain a TiO_2 film of 15 μm thickness. After cooling to 100 °C, the TiO_2 film was immersed in a dye solution (0.5 mM in DMF) and then kept at room temperature in the dark for 24 h. After drying, an electrolyte solution containing LiI (0.5 M), I_2 (0.02 M), 1-methyl-3-hexylimidazolium iodide (HMII, 0.3 M), and 4-*tert*-butylpyridine (0.5 M) in 3-methoxypropionitrile was used as the electrolyte. Pt foil was used as the counterelectrode and was clipped onto the top of the TiO_2. The dye-coated semiconductor film was illuminated through a conducting glass support without a mask. Photoelectron chemical performance of the solar cell was measured using a Keithley 2602 Source meter controlled by a computer. The cell parameters were obtained under an incident light with intensity 100 mW cm^{-2}, which was generated by a 500-W Xe lamp passing through an AM 1.5 G filter with an effective area of 0.16 cm^2.

Materials: All starting materials were obtained from Shanghai Chemical Reagent Co. Ltd. (Shanghai China) and used without further purification. All solvents used were analytical grade. 3,8-Dibromo-1,10-phenanthroline,[40,41] 3,3′-dicarboxy-2,2′-bipyridine,[42] 2,7-divinyl-9,9-dioctylfluorene[43] (**3**), and 1,4-divinyl-2-methoxyl-5-octyloxybenzene[44] (**4**) were synthesized according to the literature methods. Triethylamine was purified by distillation over KOH. DMF and THF were dried by distillation over CaH_2. All other reagents and solvents were commercially purchased and were used as received.

Synthesis of Metal Complex L1: A methanol solution (10 mL) of $Zn(CH_3COO)_2{\cdot}2H_2O$ (0.22 g, 1 mmol) was slowly dropped into a mixture of 3,8-dibromo-1,10-phenanthroline (0.338 g, 1 mmol), and 3,3′-dicarboxy-2,2′-bipyridine(0.244 g, 1 mmol) in THF (20 mL). The reaction system was neutralized carefully with NaOH (1 M) to slightly acidic pH and refluxed for 6 h. The reaction system was then cooled to room temp., filtered, washed twice with methanol and with water repeatedly, and then dried under vacuum at room temperature overnight. A white solid product was collected (0.613 g, yield 80%). FT-IR (KBr): $\tilde{\nu}$ = 3402 (OH), 3037, 3009 (Ar-CH), 1650 (C=O), 1582.4 (C=N), 1099 (C–O–M), 559 (M–N) cm^{-1}. $C_{28}H_{20}Br_2N_4O_8Zn$ (765.68): calcd. C 43.37, H 2.58, N 7.29; found C 43.92, H 2.63, N 7.32.

Synthesis of Metal Complex L2: The same synthesis method [$Co(CH_3COO)_2{\cdot}4H_2O$ (0.249 g, 1 mmol)] as described for metal complex **L1** yielded a pink–yellow solid (0.629 g 83%). FT-IR (KBr): $\tilde{\nu}$ = 3413 (=C–H), 3017 (aromatic C–H), 1631 (C=O), 1564 (C=N), 1107 (C=N–M). 554 (M–N) cm^{-1}. $C_{28}H_{20}Br_2CoN_4O_8$ (759.23): calcd. C 44.12, H 2.60, N 7.34; found C 44.30, H 2.66, N 7.38.

Synthesis of Polymeric Metal Complex P1: The polymeric metal complex **P1** was synthesized according to the literature.[31] A mixture of metal complex **L1** (0.3687 g, 0.315 mmol), 2,7-divinyl-9,9-dioctylfluorene (0.139 g, 0.315 mmol), $Pd(OAc)_2$ (0.0029 g, 0.013 mmol), triethylamine (3 mL), tri-*o*-tolylphosphane (0.022 g, 0.072 mmol) and DMF (8 mL) heated at 90 °C in the presence of nitrogen for 36 h. After the reaction mixture was cooled to room temperature and filtered, the filtrate was poured into methanol. The resulting precipitate was filtered and washed with cold methanol. The crude product was purified by dissolving it in THF and precipitating into methanol to afford a brown solid (0.19 g, 45%).

 © 2013 Wiley-VCH Verlag GmbH & Co. KGaA, Weinheim

FT-IR (KBr): $\tilde{\nu}$ = 3041 (=C–H), 2927, 2851, 1639 (C=O), 1572 (C=N), 1099 (C=N–M), 542 (N–M) cm^{-1}. $C_{63}H_{70}N_4O_8Zn$ (1076.65): calcd. C 70.61, H 6.44, N 5.36; found C 70.28, H 6.55, N 5.20. $\bar{M}_n$ = 10.1 kg/mol, PDI = 1.53.

Synthesis of Polymeric Metal Complex P2: A similar synthetic method as for **P1** was applied. A mixture of metal complex **L2** (0.2392 g, 0.315 mmol), 2,7-divinyl-9,9-dioctylfluorene (0.139 g, 0.315 mmol), $Pd(OAc)_2$ (0.0029 g, 0.013 mmol), triethylamine (3 mL), tri-*o*-tolylphosphane (0.022 g, 0.072 mmol) and DMF (8 mL) afforded a brown solid (0.14 g, 41%). FT-IR (KBr): $\tilde{\nu}$ = 3043 (=C–H), 2927, 2852, 1637 (C=N), 1560 (C=N), 1093 (C=N–M), 536 (N–M) cm^{-1}. $C_{63}H_{70}CoN_4O_8$ (1070.20): calcd. C 71.13, H 6.50, N 5.12; found C 70.70, H 6.59, N 5.24. $\bar{M}_n$ = 11.6 kg/mol, PDI = 1.76.

Synthesis of Polymeric Metal Complex P3: A similar synthetic method as for **P1** was applied. A mixture of metal complex **L1** (0.2412 g, 0.315 mmol), 1,4-divinyl-2-methoxy-5-octyloxybenzene (0.1197 g, 0.315 mmol), $Pd(OAc)_2$ (0.0029 g, 0.013 mmol), triethylamine (3 mL), tri-*o*-tolylphosphane (0.022 g, 0.072 mmol) and DMF (8 mL) afforded a pale yellow solid (0.17 g, 52%). FT-IR (KBr): $\tilde{\nu}$ = 3040 (=C–H), 2921, 2851, 1620 (C=N), 1558 (C=N),1092 (C=N–M), 531 (N–M) cm^{-1}. $C_{57}H_{70}N_4O_{10}Zn$ (1036.58): calcd. C 65.77, H 6.95, N 5.42; found C 66.05, H 6.81, N 5.40, $\bar{M}_n$ = 11.8 kg/mol, PDI = 1.26.

Synthesis of Polymeric Metal Complex P4: A similar synthetic method as for **P1** was applied. A mixture of metal complex **L2** (0.2392 g, 0.315 mmol), 1,4-divinyl-2-methoxy-5-octyloxybenzene (0.1197 g, 0.315 mmol), $Pd(OAc)_2$ (0.0029 g, 0.013 mmol), triethylamine (3 mL), tri-*o*-tolylphosphane (0.022 g, 0.072 mmol) and DMF (8 mL) afforded an orange-yellow solid (0.16 g, 48%). FT-IR (KBr): $\tilde{\nu}$ = 3039 (=C–H), 2923, 2850, 1630 (C=O), 1571 (C=N), 1096 (C=N–M), 547 (N–M) cm^{-1}. $C_{57}H_{70}CoN_4O_{10}$ (1030.13): calcd. C 66.70, H 6.73, N 5.42; found C 66.46, H 6.85, N 5.44. $\bar{M}_n$ = 14.8 kg/mol, PDI = 1.64.

Supporting Information (see footnote on the first page of this article): Synthesis and ^1H NMR spectra of compounds **1**–**4**.

Acknowledgments

The authors thank the Ministry of Education, China for financial support through the Open Project Program of Key Laboratory of Environmentally Friendly Chemistry and Applications (No. 09HJYH10). Thanks to all the co-workers who worked on polymeric metal complex in our laboratory.

[1] X. Jiang, K. M. Karlsson, E. Gabrielsson, E. M. J. Johansson, M. Quintana, M. Karlsson, L. Sun, G. Boschloo, A. Hagfeldt, *Adv. Funct. Mater.* **2011**, *21*, 2944–2952.
[2] B. Oregan, M. Grätzel, *Nature* **1991**, *353*, 737–739.
[3] Y. Ooyama, Y. Harima, *Eur. J. Org. Chem.* **2009**, *18*, 2903–2934.
[4] M. Katono, T. Bessho, M. Wielopolski, M. Marszalek, J.-E. Moser, R. Humphry-Baker, S. M. Zakeeruddin, M. Grätzel, *J. Phys. Chem. C* **2012**, *116*, 16876–16884.
[5] M. K. Nazeeruddin, A. Kay, I. Rodicio, R. Humphrybaker, E. Muller, P. Liska, N. Vlachopoulos, M. Grätzel, *J. Am. Chem. Soc.* **1993**, *115*, 6382–6390.
[6] M. K. Nazeeruddin, S. M. Zakeeruddin, R. Humphry-Baker, M. Jirousek, P. Liska, N. Vlachopoulos, V. Shklover, C. H. Fischer, M. Grätzel, *Inorg. Chem.* **1999**, *38*, 6298–6305.
[7] Z. S. Wang, T. Yamaguchi, H. Sugihara, H. Arakawa, *Langmuir* **2005**, *21*, 4272–4276.
[8] P. Wang, C. Klein, R. Humphry-Baker, S. M. Zakeeruddin, M. Grätzel, *J. Am. Chem. Soc.* **2005**, *127*, 808–809.
[9] F. Gao, Y. Wang, D. Shi, J. Zhang, M. K. Wang, X. Y. Jing, R. Humphry-Baker, P. Wang, S. M. Zakeeruddin, M. Grätzel, *J. Am. Chem. Soc.* **2008**, *130*, 10720–10728.
[10] C. Y. Chen, M. K. Wang, J. Y. Li, N. Pootrakulchote, L. Alibabaei, C. H. Ngoc-le, J. D. Decoppet, J. H. Tsai, C. Grätzel, C. G. Wu, S. M. Zakeeruddin, M. Grätzel, *ACSNano* **2009**, *3*, 3103–3109.
[11] A. Yella, H. W. Lee, H. N. Tsao, C. Yi, A. K. Chandiran, M. K. Nazeeruddin, M. Grätzel, *Science* **2011**, *334*, 629–634.
[12] H. T. Chan, C. S. K. Mak, A. B. Djurišić, W. K. Chan, *Macromol. Chem. Phys.* **2011**, *212*, 774–784.
[13] X. Ren, S. Jiang, M. Cha, G. Zhou, Z. S. Wang, *Chem. Mater.* **2012**, *24*, 3493–3499.
[14] A. Dualeh, F. De Angelis, S. Fantacci, T. Moehl, C. Yi, F. Kessler, E. Baranoff, M. K. Nazeeruddin, M. Grätzel, *J. Phys. Chem. C* **2012**, *116*, 1572–1578.
[15] C. Wang, H. Dong, W. Hu, Y. Liu, D. Zhu, *Chem. Rev.* **2012**, *112*, 2208–2267.
[16] Z. Chen, F. Li, C. Huang, *Curr. Org. Chem.* **2007**, *11*, 1241–1258.
[17] Y. J. Liu, X. Guo, N. Xiang, B. Zhao, H. Huang, H. Li, P. Shen, S. Tan, *J. Mater. Chem.* **2010**, *20*, 1140–1146.
[18] Y. Tang, P. Shen, T. Ding, H. Huang, B. Zhao, S. Tan, *Eur. Polym. J.* **2010**, *46*, 2033–2041.
[19] Y. J. Cheng, S. H. Yang, C. S. Hsu, *Chem. Rev.* **2009**, *109*, 5868–5871.
[20] M. R. Bryce, *Adv. Mater.* **1999**, *11*, 11–23.
[21] Y. Shen, B. P. Sullivan, *Inorg. Chem.* **1995**, *34*, 6235–6236.
[22] J. F. Yin, D. Bhattacharya, Y. C. Hsu, C. C. Tsai, K. L. Lu, H. C. Lin, J. G. Chen, K. C. Ho, *J. Mater. Chem.* **2009**, *19*, 7036–7042.
[23] K. Hara, H. Sugihara, L. P. Singh, A. Islam, R. Katoh, M. Yanagida, K. Sayama, S. Murata, H. Arakawa, *J. Photochem. Photobiol. A: Chem.* **2001**, *145*, 117–122.
[24] C. Y. Chen, H. C. Lu, C. G. Wu, J. G. Chen, K. C. Ho, *Adv. Funct. Mater.* **2007**, *17*, 29–36.
[25] B. Wu, H.-Q. Zhang, H.-Y. Zhang, Q. Wu, H. Hou, Y. Zhu, X. Wang, *Syn. React. Inorg. Met-Org. Chem.* **2004**, *34*, 313–321.
[26] R. F. Heck, J. P. Nolley, *J. Org. Chem.* **1972**, *37*, 2320–2322.
[27] G. Robert, H. Charles, R. Freiser, L. Friedel, E. Hilliard, W. D. Johnston, *Spectochimica. Acta* **1956**, *8*, 1–8.
[28] R. Pagadala, P. Ali, J. S. Meshram, *J. Coord. Chem.* **2009**, *62*, 4009–4017.
[29] Y. Liu, Q. Xiu, L. Xiao, H. Huang, L. Guo, L. Zhang, H. Zhang, S. Tan, C. Zhong, *Polym. Adv. Technol.* **2011**, *22*, 2583–2591.
[30] S. C. Ng, J. M. Xu, H. S. O. Chan, *Synth. Met.* **2000**, *110*, 31–36.
[31] *Organic PhotoVoltaics: Mechanisms, Materials and Devices* (Eds.: S. S. Sun, N. S. Sariciftci), CRC, Boca Raton, **2005**, vol. 3, p. 217–239.
[32] S. Tokito, H. Tanaka, K. Noda, A. Okada, Y. Taga, *Appl. Phys. Lett.* **1997**, *70*, 1929–1931.
[33] N. S. Cho, D. H. Hwang, B. J. Jung, E. Lim, J. Lee, H. K. Shim, *Macromolecules* **2004**, *37*, 5265–5273.
[34] Y. Li, Y. Cao, J. Gao, D. Wang, G. Yu, A. J. Heeger, *Synth. Met.* **1999**, *99*, 243–248.
[35] P. Qin, X. Yang, R. Chen, L. Sun, T. Marinado, T. Edvinsson, G. Boschloo, A. Hagfeldt, *J. Phys. Chem. C* **2007**, *111*, 1853–1860.
[36] G. L. Zhang, B. H, Y. M. Cheng, D. Shi, X. J. Lv, Q. J. Yu, P. Wang, *Chem. Commun.* **2009**, *45*, 2198–2200.
[37] Z. S. Wang, K. Sayama, H. Sugihara, *J. Phys. Chem. B* **2005**, *109*, 22449–22455.
[38] B. Kraabel, D. McBranch, N. S. Sariciftci, D. Moses, A. J. Heeger, *Phys. Rev. B* **1994**, *50*, 18543–18552.

 © 2013 Wiley-VCH Verlag GmbH & Co. KGaA, Weinheim

[39] S. F. J. Garín, N. M. Baroja, R. P. Tejada, J. Orduna, Y. Yu, M. L. Cantú, *Org. Lett.* **2012**, *14*, 752–755.
[40] Y. Saitoh, T. Koizumi, K. Osakada, T. Yamamoto, *Can. J. Chem.* **1997**, *75*, 1336–1339.
[41] T. Yamamoto, K. Anzai, H. Fukumoto, *Chem. Lett.* **2002**, *31*, 774–776.
[42] B. Z. Shan, Q. Zhao, N. Goswami, D. M. Eichhorn, D. P. Rillema, *Coord. Chem. Rev.* **2001**, *211*, 117–144.
[43] L. R. Tsai, C. W. Li, Y. J. Chen, *J. Polym. Sci., Part A: Polym. Chem.* **2008**, *46*, 5945–5958.
[44] K. Liu, Y. Li, M. J. Yang, *J. Appl. Polym. Sci.* **2009**, *111*, 1976–1984.

Received: February 22, 2013
Published Online: July 29, 2013

 © 2013 Wiley-VCH Verlag GmbH & Co. KGaA, Weinheim